Comput. Methods Appl. Mech. Engrg. 255 (2013) 147–157

Contents lists available at SciVerse ScienceDirect

Comput. Methods Appl. Mech. Engrg.

journal homepage: www.elsevier.com/locate/cma

# Non-linear Petrov–Galerkin methods for reduced order modelling of the Navier–Stokes equations using a mixed finite element pair

D. Xiao [a,b], F. Fang [b], J. Du [d], C.C. Pain [b], I.M. Navon [c,*], A.G. Buchan [b], A.H. ElSheikh [b], G. Hu [a]

[a] State Key Laboratory of Geological Processes and Mineral Resources, China University of Geosciences, Wuhan 430074, China
[b] Applied Modelling and Computation Group, Department of Earth Science and Engineering, Imperial College London, Prince Consort Road, London SW7 2AZ, UK
[c] Department of Scientific Computing, Florida State University, Tallahassee, FL 32306-4120, USA
[d] Institute of Atmospheric Physics, Chinese Academy of Sciences, Beijing 100029, China

ARTICLE INFO

*Article history:*
Received 11 June 2012
Received in revised form 3 November 2012
Accepted 8 November 2012
Available online 29 November 2012

*Keywords:*
Finite element
Petrov–Galerkin
Navier–Stokes
Proper orthogonal decomposition
Discontinuous-Galerkin

ABSTRACT

A new nonlinear Petrov–Galerkin approach has been developed for proper orthogonal decomposition (POD) reduced order modelling (ROM) of the Navier–Stokes equations. The new method is based on the use of the cosine rule between the advection direction in Cartesian space–time and the direction of the gradient of the solution. A finite element pair, $P_{1DG}P_2$, which has good balance preserving properties is used here, consisting of a mix of discontinuous (for velocity components) and continuous (for pressure) basis functions. The contribution of the present paper lies in applying this new non-linear Petrov–Galerkin method to the reduced order Navier–Stokes equations, and thus improving the stability of ROM results without tuning parameters. The results of numerical tests are presented for a wind driven 2D gyre and the flow past a cylinder, which are simulated using the unstructured mesh finite element CFD model in order to illustrate the numerical performance of the method. The numerical results obtained show that the newly proposed POD Petrov–Galerkin method can provide more accurate and stable results than the POD Bubnov–Galerkin method.



## 1. Introduction

The proper orthogonal decomposition (POD)/Galerkin method has been used extensively for reduced order models (ROMs). The POD method optimally extracts the few most energetic modes/bases from the numerical/experimental solutions that can accurately represent the system dynamics. The POD approach was introduced in 1901, referred then as Principal Component Analysis (PCA) by Pearson [1]. Later work includes [2,3] in statistics, or empirical orthogonal functions (EOF) in oceanography, [4] and meteorology [5]. The POD methods, in combination with the Galerkin projection procedure, have also provided an efficient means for generating reduced-order models [6–8]. In POD reduced order modelling, the Galerkin method is used to project the original equations onto a finite number of POD bases and yields a set of ordinary differential equations in time. POD has been used successfully in several fields, such as fluid dynamics [9–11], signal processing and pattern recognition [3], inverse problems [12,13] and ocean modelling and four-dimensional variational (4D-Var) data assimilation [14–17].

However, the POD/Galerkin finite element model (FEM) lacks stability and spurious oscillations can degrade the reduced order solution for flows with high Reynolds numbers [18]. The instabilities commonly observed in the POD method are due to oscillations forming in the solutions as a result of applying a standard Bubnov–Galerkin projection of the equations onto the reduced order space. This is very similar to the oscillations that form in FEM solutions when the standard Bubnov–Galerkin method is applied. These oscillations feed into the non-linear terms at moderate to high Reynolds numbers resulting in unstable simulations. In this paper, stable results are obtained by using a suitable Petrov–Galerkin projection with ROM. Various methods have been developed to overcome the POD stability problem. Iollo et al. [10] succeeded in stabilising the POD/Galerkin approximation of the Navier–Stokes equations by employing numerical dissipation. The numerical stability of the ROM is also related to the choice of the inner product used to define the Galerkin projection. A stable symmetrical inner product that guarantees certain stability bounds for the linearised compressible Euler equations was proposed by Kalashnikova and Barone [19]. Angelo et al. [20,21] proposed two

* Corresponding author. Tel.: +1 850 644 6560; fax: +1 850 644 0098 (I.M. Navon).
*E-mail address:* inavon@fsu.edu, inavon@scs.fsu.edu (I.M. Navon).
*URLs:* http://amcg.ese.imperial.ac.uk (D. Xiao), http://amcg.ese.imperial.ac.uk (F. Fang), http://amcg.ese.imperial.ac.uk (C.C. Pain), http://www.sc.fsu.edu/~inavon (I.M. Navon), http://amcg.ese.imperial.ac.uk (A.G. Buchan), http://amcg.ese.imperial.ac.uk (A.H. ElSheikh).

0045-7825/$ - see front matter © 2012 Elsevier B.V. All rights reserved.
http://dx.doi.org/10.1016/j.cma.2012.11.002

stabilization methods for POD/ROM: one that relies on the explicit addition of an artificial dissipation term whose construction is similar to that of the Lax–Wendroff scheme; another one that consists in constructing the POD for both function and gradient values (POD in $H_1$) (calibration). Another type of regularization is found to improve the stability of the POD/Galerkin models of strongly-stiff systems [22]. The method replaces the POD eigenmodes of the non-linear terms by their Helmholtz filtered counterparts, while the other terms remain unchanged.

Another difficulty that arises in applying the POD/Galerkin method to nonlinear fluid problems involves the efficient computation of the projection of the nonlinear terms that are present in the equations. Recently, several approaches have been proposed for retaining the intended efficiency of $O(M)$ (where $M$ is the number of reduced basis modes) of the ROM, instead of $O(N)$ (where $N$ is the number of grid-points in the full high-fidelity simulation). Chaturantabut and Sorensen [23] proposed a non-linear model reduction via the discrete empirical interpolation method (DEIM) [25,26], which is the discrete version of the empirical interpolation method (EIM) [24]. This method was applied by these authors in conjunction with POD to treat the reduction of non-linear miscible viscous fingering in porous media [27], and derived state space error bounds for the solutions of POD/DEIM [28]. Another similar technique for non-linear treatments is the best points interpolation method (BPIM) [29]. Nguyen and Peraire [30] also addressed the issue for the reduction of the non-linear elliptic equation and highly non-linear time-dependent convection–diffusion equations through the reduced basis approximation (RBA) technique. For such classes of FEM PDEs, the reduced-order modelling provided by the standard Galerkin projection is no longer efficient. This is because the evaluation of the integrals involving the non-affine and non-linear terms is computationally expensive and cannot be pre-computed [30]. The RBA technique does vary from the standard POD method but does use the EIM in its formulation. A comparison of a number of POD formulations including the greedy reduced order approximation (ROA), the reduced-basis approach (RBA) of [24,31] and the standard Galerkin projection approach has been provided in [30].

Recently, Carlberg et al. introduced the Petrov–Galerkin method to control the stability of reduced order modelling of a 1D nonlinear static problem [32,33]. This method offers a natural and easy way to introduce a diffusion term into ROM without requiring tuning/optimising and provides appropriate modelling and stabilisation for the POD numerical solution. More recently, a new Petrov–Galerkin method for reduced order modelling has been proposed for nonlinearly discontinuous Galerkin modelling in order to control numerical oscillations, and applied to nonlinear hyperbolic problems [34]. The approach is based on the use of the cosine rule between the advection direction in Cartesian space–time and the solution gradient direction.

In the present work, the new Petrov–Galerkin method [34] is used for the stabilisation of reduced order modelling of a nonlinear hybrid unstructured mesh model which is applied to the Navier–Stokes equations. A mixed $P_{1DG}P_2$ finite element pair [35] which remains Ladyzanskya Babuska Brezzi (LBB) stable and has good balance preserving properties, is introduced here to further stabilise the numerical oscillation. It consists of discontinuous linear elements for velocity and continuous quadratic elements for pressure in the Navier–Stokes equations [36,38]. To efficiently treat the non-linear components of the equation, we have used the method proposed in [39], which assumes that the system of discrete equations are quadratic. This is an approximation but is motivated by the observation that the continuous PDE (the Navier–Stokes equations) has a quadratic non-linearity and thus can be discretized using a quadratic discrete system of equations. The CPU cost of this is $O(M^3)$ per time step, and since the magnitude of $M$ is relatively small the method is highly efficient.

The remainder of the paper is organised as follows. Section 2 introduces the governing equations used in this work. Section 3 presents the derivation of the new Petrov–Galerkin approach for a single scalar time dependent transport equation, and this is then extended to a set of coupled time dependent equations in Section 4. Section 5 provides the derivation of reduced order modelling of Navier–Stokes equations using the newly proposed Petrov–Galerkin approach. In Section 6, the novel reduced order nonlinear hybrid unstructured mesh model is applied to two test cases, namely, a wind driven 2D Gyre and flow past a cylinder. Finally, the summary and conclusions of this article are presented in Section 7.

## 2. Governing equations

The underlying model equations used here consist of the 3-D non-hydrostatic Navier–Stokes equations:

$$\nabla \cdot \mathbf{u} = 0, \tag{1}$$

$$\frac{\partial \mathbf{u}}{\partial t} + \mathbf{u} \cdot \nabla \mathbf{u} + f\mathbf{k} \times \mathbf{u} = -\nabla p + \nabla \cdot \boldsymbol{\tau}, \tag{2}$$

where $\mathbf{u} \equiv (u, v, w)^T \equiv (u_1, u_2, u_3)^T$ is the velocity vector, $p$ is the perturbation pressure ($p := p/\rho_0$, $\rho_0$ is the constant reference density), $f$ represents the Coriolis inertial force, and $\mathbf{k}$ is an unit vector along the vertical direction. The stress tensor $\boldsymbol{\tau}$ in the diffusion term is used to represent the viscous terms and is defined in terms of the deformation rate tensor $\mathbf{S}$ as

$$\tau_{ij} = 2\mu_{ij}S_{ij}, \quad S_{ij} = \frac{1}{2}\left(\frac{\partial u_i}{\partial x_j} + \frac{\partial u_j}{\partial x_i}\right) - \frac{1}{3}\sum_{k=1}^{3}\frac{\partial u_k}{\partial x_k}, \quad 1 \leqslant i, j \leqslant 3, \tag{3}$$

where, $\mu$ is the kinematic viscosity. In the previous definition, we assume no summation over repeated indices. In this paper, the horizontal kinematic viscosities ($\mu_{11}$, $\mu_{22}$) and vertical kinematic viscosity ($\mu_{33}$) take constant values with the off-diagonal components of $\boldsymbol{\tau}$ defined by $\mu_{ij} = (\mu_{ii}\mu_{jj})^{1/2}$. For barotropic flow, the pressure $p$ consists of hydrostatic $p_h(z)$ and non-hydrostatic $p_{nh}(x, y, z, t)$ components. The hydrostatic component of pressure balances exactly the constant buoyancy force and both terms are therefore neglected at this stage.

The momentum equation discretised in space can be rewritten in a matrix form:

$$A_t\frac{\partial \mathbf{u}}{\partial t} + A_x(\mathbf{u})\frac{\partial \mathbf{u}}{\partial x} + A_y(\mathbf{u})\frac{\partial \mathbf{u}}{\partial y} + A_z(\mathbf{u})\frac{\partial \mathbf{u}}{\partial z} + f\mathbf{k} \times \mathbf{u} + \nabla p - \nabla \cdot \boldsymbol{\tau} = 0, \tag{4}$$

where

$$A_t = \begin{pmatrix} 1 & 0 & 0 \\ 0 & 1 & 0 \\ 0 & 0 & 1 \end{pmatrix}, \tag{5}$$

$$A_x = \begin{pmatrix} u & 0 & 0 \\ 0 & u & 0 \\ 0 & 0 & u \end{pmatrix}, \quad A_y = \begin{pmatrix} v & 0 & 0 \\ 0 & v & 0 \\ 0 & 0 & v \end{pmatrix}, \quad A_z = \begin{pmatrix} w & 0 & 0 \\ 0 & w & 0 \\ 0 & 0 & w \end{pmatrix}. \tag{6}$$

## 3. A scalar Petrov–Galerkin transport equation

In order to derive the newly proposed Petrov–Galerkin approach, the outline for a scalar time dependent transport equation is derived first. The scalar time dependent transport equation used is:

$$\mathbf{a}_{xt} \cdot \nabla_{xt}\psi + \sigma\psi = s, \tag{7}$$

where $\psi$ represents field states (e.g. temperature, pollutants) and $s$ is the source term; for 1D: $\mathbf{a}_{xt} = (\,a_t \quad a_x\,)^T$, for 2D: $\mathbf{a}_{xt} = (\,a_t \quad a_x \quad a_y\,)^T$ and for 3D: $\mathbf{a}_{xt} = (\,a_t \quad a_x \quad a_y \quad a_z\,)^T$ and in 2D with time dependence this equation assumes the form:

$$a_t \frac{\partial \psi}{\partial t} + a_x \frac{\partial \psi}{\partial x} + a_y \frac{\partial \psi}{\partial y} + \sigma\psi - s = 0. \tag{8}$$

Using the cosine rule between the two vectors $\mathbf{a}_{xt}$ and $\nabla_{xt}\psi$, in which $\theta_a$ is the angle between the two vectors, then:

$$cos\theta_a = \frac{\mathbf{a}_{xt} \cdot \nabla_{xt}\psi}{|\,\mathbf{a}_{xt}\,|\,|\,\nabla_{xt}\psi\,|} \tag{9}$$

and the projection of $\mathbf{a}_{xt}$ onto $\nabla_{xt}\psi$ may be written as $\mathbf{a}^*_{xt} = |\,\mathbf{a}_{xt}\,|\,\mathbf{n}_a cos(\theta_a)$ (with $\mathbf{n}_a = \frac{\nabla_{xt}\psi}{|\nabla_{xt}\psi|}$) or in the detailed form:

$$\mathbf{a}^*_{xt} = \frac{(\mathbf{a}_{xt} \cdot \nabla_{xt}\psi)\nabla_{xt}\psi}{\|\,\nabla_{xt}\psi\|^2}. \tag{10}$$

Thus

$$\mathbf{a}^*_{xt} \cdot \nabla_{xt}\psi = \mathbf{a}_{xt} \cdot \nabla_{xt}\psi \tag{11}$$

or

$$\left(\frac{(\mathbf{a}_{xt} \cdot \nabla_{xt}\psi)\nabla_{xt}\psi}{\|\nabla_{xt}\psi\|^2}\right) \cdot \nabla_{xt}\psi = \mathbf{a}_{xt} \cdot \nabla_{xt}\psi. \tag{12}$$

A Petrov–Galerkin approach is used that modifies the governing equation by its weighting with a stabilisation term. This is given by the equation,

$$(1 - \nabla_{xt} \cdot \mathbf{a}^*_{xt} p^*_{xt})(\mathbf{a}_{xt} \cdot \nabla_{xt}\psi + \sigma\psi - s) = 0, \tag{13}$$

where the scalar $p^*_{xt}$ is a function of $\mathbf{a}^*_{xt}$ and the size and shape of the elements (to be later defined in (16)–(18)). Eq. (13) is a consistent formulation which stabilizes the solution by adding artificial diffusion in the direction of its gradient. This effectively smooths out the unphysical oscillations that form in extreme regimes, such as in high Reynolds numbers. This technique is now a commonly used method for stabilising finite element solution and its origins date back to the work in [40–43]. Multiplying Eq. (13) by a space–time basis function $N_{xti}$ and integrating over a single element $V_E$ with boundary $\Gamma_E$ and applying integration by parts results in:

$$\int_{V_E} N_{xti} r dV_E - \int_{\Gamma_E} N_{xti}(\mathbf{n}_{xt} \cdot \mathbf{a}_{xt})(\psi - \psi_{bc})\, d\Gamma_E + \int_{V_E} (\nabla_{xt} N_{xti}) \cdot \mathbf{a}^*_{xt} p^*_{xt} r\, dV_E + \int_{\Gamma_E} N_{xti} \mathbf{n}_{xt} \cdot \mathbf{a}^*_{xt} p^*_{xt} r\, d\Gamma_E = 0. \tag{14}$$

In this formulation the term $r$ is the residual, which is expressed as $r = \mathbf{a} \cdot \nabla_{xt}\psi + \sigma\psi - s$, and the term $\mathbf{n}_{xt}$ is the unit vector that is normal to the element in space–time. In this work the boundary information $\psi_{bc}$ is treated in an upwind fashion. That is, if $\mathbf{n}_{xt} \cdot \mathbf{a}_{xt}$ is negative then $\psi_{bc}$ takes on the values of the neighbouring elements. Alternatively if $\mathbf{n}_{xt} \cdot \mathbf{a}_{xt}$ is positive then the values within the element are used. The approximation of $\psi$ will now be assumed to be expressed as a finite element expansion, $\psi = \sum_{j=1}^{\mathcal{N}} N_{xtj}\psi_j$. Finally, the surface integral involving the residual is assumed to be zero, and this results in the following formulation,

$$\int_{V_E} N_{xti} r dV_E - \int_{\Gamma_E} (\mathbf{n}_{xt} \cdot \mathbf{a}_{xt}) N_{xti}(\psi - \psi_{bc}) d\Gamma_E + \int_{V_E} (\nabla_{xt} N_{\,xti}) \cdot \mathbf{a}^*_{xt} p^*_{xt} r dV_{\,E} = 0. \tag{15}$$

The scalar $p^*_{xt}$ which a function of $\mathbf{a}^*_{xt}$ and the size and shape of the elements, is given, for example, by the following expression:

$$p^*_{xt} = \frac{1}{4}(\,|\,\mathbf{a}^*_{xt} \cdot \nabla_{xt} N_{\,xti}\,|\,)^{-1}. \tag{16}$$

This expression is obtained from the Riemann finite element method, for details see [44]. This will choose the shape function which is aligned with the direction of $\mathbf{a}^*_{xt}$, for example, in the case for elements with equal sized edges.

Alternatively one can produce a $p^*_{xt}$ that is independent of $i$ using:

$$p^*_{xt} = min_k\left\{\frac{1}{4}(\,|\,\mathbf{a}^*_{xt} \cdot \nabla_{xt} N_{xtk}\,|\,)^{-1}\right\}. \tag{17}$$

Notice that this expression uses the length scale of the element in the direction of $\mathbf{a}^*_{xt}$.

Using the L2-norm and the finite element space–time Jacobian matrix $\mathbf{J}_{xt}$ (see Eq. (40)), an alternative expression to (17) has the following form:

$$p^*_{xt} = \frac{1}{4}(\|\mathbf{J}^{-1}_{xt}\mathbf{a}^*_{xt}\|_2)^{-1}. \tag{18}$$

The value of $p^*_{xt}$ can be adjusted in order to ensure that the resulting value of $p^*_{xt}$ is not so large that it results in having more transport backward than forward in the resulting discrete system of equations by using:

$$p^*_{xt} = min\left\{\frac{1}{\sigma + \epsilon}, \frac{1}{4}(\|\mathbf{J}^{-1}_{xt}\mathbf{a}^*_{xt}\|_2)^{-1}\right\}, \tag{19}$$

in which $\sigma + \epsilon > 0$ and $\epsilon$ is a small positive number that ensures we avoid dividing by zero $\sigma = 0$ e.g. $\epsilon = 1 \times 10^{-10}$.

Continuous Petrov–Galerkin formulations use a factor of $\frac{1}{2}$ instead of $\frac{1}{4}$ as used in the previous equations. This correctly centres the equation residual at the centre of mass of the basis function, for continuous finite element representations. In the present work, where discontinuous finite elements are used to formulate the space–time discretisation, the centre of mass of the basis function is centred at a distance of $\frac{\Delta x}{4}$ from the upwind boundary of the element. In the traditional Petrov–Galerkin method $\mathbf{a}^*_{xt} = \mathbf{a}_{xt}$ in the aforementioned expression and $p_{xt}$ replaces $p^*_{xt}$.

We can work with the stabilization in a diffusion form by using:

$$\int_{V_E} N_{xti} r dV_E - \int_{\Gamma_E} N_{xti}(\mathbf{n}_{xt} \cdot \mathbf{a}_{xt})(\psi - \psi_{bc}) d\Gamma_E + \int_{V_E} (\nabla_{xt} N_{xti})^T \nu \nabla_{xt}\psi dV_E = 0, \tag{20}$$

in which the scalar diffusion coefficient is:

$$\nu = \frac{(\mathbf{a}_{xt} \cdot \nabla_{xt}\psi)p^*_{xt} r}{\|\nabla_{xt}\psi\|^2}. \tag{21}$$

Alternatively, we can work only on the residual. That is, replacing $\mathbf{a}_{xt} \cdot \nabla_{xt}\psi$ with the residual $r$ in (21), yields:

$$\nu = \frac{r p^*_{xt} r}{\|\nabla_{xt}\psi\|^2}. \tag{22}$$

The diffusion coefficient $\nu$ is always non-negative since $p^*_{xt}$ is non-negative. Eq. (22) for the diffusivity can be derived by re-defining the term $\mathbf{a}^*_{xt}$ in Eq. (10) to be:

$$\mathbf{a}^*_{xt} = \frac{r\nabla_{xt}\psi}{\|\nabla_{xt}\psi\|^2}. \tag{23}$$

Then $\mathbf{a}^*_{xt} \cdot \nabla_{xt}\psi = \frac{r\nabla_{xt}\psi}{\|\nabla_{xt}\psi\|^2} \cdot \nabla_{xt}\psi = r$.

### 3.1. Simplified scalar equation

Discretising the time dependent term using the two level $\theta$-method, the residual becomes:

$$r = a_t \frac{\psi^{n+1} - \psi^n}{\Delta t} + \mathbf{a} \cdot \nabla\psi^{n+\theta} + \sigma\psi^{n+\theta} - s^{n+\theta}, \tag{24}$$

with $\mathbf{a} = (\,a_x \quad a_y \quad a_z\,)^T$ and $\psi^{n+\theta} = \theta\psi^{n+1} + (1-\theta)\psi^n$ also defining

$$\nabla_{xt}\psi = \left(\frac{\psi^{n+1}-\psi^n}{\Delta t},\ (\nabla\psi^{n+\theta})^T\right)^T. \tag{25}$$

Using this definition (Eq. (25)) enables the formalism of space–time discretisation to be applied, for example:

$$\mathbf{a}^*_{xt} = (a^*_t,\ \mathbf{a}^{*T})^T = \frac{(\mathbf{a}_{xt}\cdot\nabla_{xt}\psi)\nabla_{xt}\psi}{\|\nabla_{xt}\psi\|_2^2} \tag{26}$$

and

$$\mathrm{p}^*_{xt} = min\left\{\frac{1}{\sigma+\epsilon}, \frac{1}{4}(\|\mathbf{J}^{-1}\mathbf{a}^*\|_2)^{-1}\right\}, \tag{27}$$

in which $\mathbf{J}$ is the block part of the matrix $\mathbf{J}_{xt}$ that is associated with Cartesian space. The stabilized discrete equations in a diffusion form can be expressed by only using the diffusion in Cartesian space:

$$\int_{V_E} N_i r dV - \int_{\Gamma_E} N_i(\mathbf{n}\cdot\mathbf{a})(\psi^{n+\theta}-\psi^{n+\theta}_{bc})d\Gamma + \int_{V_E}(\nabla N_i)^T\nu\nabla\psi^{n+1}dV = 0 \tag{28}$$

or in a form where we apply integration by parts of the transport terms once:

$$\int_{V_E} N_i\left(a_t\left(\frac{\psi^{n+1}-\psi^n}{\Delta t}\right)+\sigma\psi^{n+\theta}-s^{n+\theta}\right)dV_E - \int_{V_E}\nabla\cdot(N_i\mathbf{a})\psi^{n+\theta}dV \tag{29}$$

$$+\int_{\Gamma_E} N_i(\mathbf{n}\cdot\mathbf{a})(\psi^{n+\theta}_{bc})d\Gamma_E + \int_{V_E}(\nabla N_i)^T\nu\nabla\psi^{n+1}dV_E = 0. \tag{30}$$

## 4. Nonlinear time dependent equations

### 4.1. The Petrov–Galerkin Navier–Stokes equations

The Petrov–Galerkin method discussed above is further applied to the Navier–Stokes equation (2), which can be rewritten as:

$$\mathbf{A}_{xt}\cdot\nabla_{xt}\mathbf{u} = \mathbf{s}, \tag{31}$$

in which $\mathbf{A}_{xt} = (\,\mathbf{A}_t \quad \mathbf{A}_x \quad \mathbf{A}_y \quad \mathbf{A}_z\,)^T$ and $\mathbf{s} = -f\mathbf{k}\times\mathbf{u} - \nabla p + \nabla\cdot\boldsymbol{\tau}$. The projection of $\mathbf{A}_{xt}$ onto $\nabla_{xt}\mathbf{u}$ can be written as:

$$\mathbf{A}^*_{xt} = \mathbf{V}(\mathbf{A}_{xt}\cdot\nabla_{xt}\mathbf{u})\mathbf{V}(\|\nabla_{xt}\mathbf{u}\|_2^2)^{-1}\nabla_{xt}\mathbf{u}. \tag{32}$$

Thus

$$\mathbf{A}^*_{xt}\cdot\nabla_{xt}\mathbf{u} = \mathbf{A}_{xt}\cdot\nabla_{xt}\mathbf{u} \tag{33}$$

or

$$\left(\mathbf{V}(\mathbf{A}_{xt}\cdot\nabla_{xt}\mathbf{u})\mathbf{V}(\|\nabla_{xt}\mathbf{u}\|_2^2)^{-1}\nabla_{xt}\mathbf{u}\right)\cdot\nabla_{xt}\mathbf{u} = \mathbf{A}_{xt}\cdot\nabla_{xt}\mathbf{u}, \tag{34}$$

in which $\mathbf{V}(\mathbf{A}_{xt}\cdot\nabla_{xt}\mathbf{u})$ is a diagonal matrix containing $\mathbf{A}_{xt}\cdot\nabla_{xt}\mathbf{u}$, and the vector $\|\nabla_{xt}\mathbf{u}\|_2^2$ is such that the $\mu$th entry is $\|\nabla_{xt}\mathbf{u}\|^2_{2\mu} = (\nabla_{xt}\mathbf{u}_\mu)\cdot(\nabla_{xt}\mathbf{u}_\mu)$.

The Petrov–Galerkin method's modified form of the differential equation is [34]:

$$(\mathbf{I} - (\nabla_{xt}\cdot\mathbf{A}^*_{xt})^T\mathbf{P}^*_{xt})(\mathbf{A}_{xt}\cdot\nabla_{xt}\mathbf{u}) - \mathbf{s} = \mathbf{0}, \tag{35}$$

where $\mathbf{P}^*_{xt}$ is a function of $\mathbf{A}^*_{xt}$ and the size and shape of the elements (see Eqs. (38) and (39)). Multiplying Eq. (35) by a diagonal matrix of space–time basis function $\mathbf{N}_{xti}$ (this has the basis function $N_{xti}$ along its main diagonal), integrating over a single element $V_E$ and applying integration by parts results in:

$$\int_{V_E}\mathbf{N}_{xti}\mathbf{r}\,dV_E - \int_{\Gamma_E}\mathbf{N}_{xti}(\mathbf{n}_{xt}\cdot\mathbf{A}_{xt})(\Psi-\Psi_{bc})\,d\Gamma_E$$

$$+\int_{V_E}((\nabla_{xt}\mathbf{N}_{xti})\cdot\mathbf{A}^*_{xt})^T\mathbf{P}^*_{xt}\mathbf{r}dV + \int_{\Gamma_E}\mathbf{N}_{xti}\mathbf{n}_{xt}\cdot\mathbf{A}^*_{xt}\mathbf{P}^*_{xt}\mathbf{r}\,d\Gamma_E = \mathbf{0}, \tag{36}$$

with a finite element expansion $\mathbf{u} = \sum_{j=1}^{\mathcal{N}}\mathbf{N}_{xtj}\mathbf{u}_j$ (where $\mathbf{u}_j$ is the velocity vector at node $j$) and $\mathbf{r} = \mathbf{A}_{xt}\cdot\nabla_{xt}\mathbf{u} - \mathbf{s}$. In this work, only the incoming information is taken into account, that is, if $\mathbf{n}_{xt}\cdot\mathbf{A}_{xt}$ is negative, then $\Psi_{bc}$ is calculated from the neighbour element (otherwise, it is calculated from the current elements). Applying a zero boundary condition for the residual $\mathbf{r} = \mathbf{0}$, yields:

$$\int_{V_E}\mathbf{N}_{xti}\mathbf{r}dV_E + \int_{V_E}(\nabla_{xt}\mathbf{N}_{xti})\cdot\mathbf{A}^*_{xt})^T\mathbf{P}^*_{xt}rdV_E = \mathbf{0}. \tag{37}$$

$\mathbf{P}^*_{xt}$ is a function of $\mathbf{A}^*_{xt}$ and the size and shape of the elements, for example:

$$\mathbf{P}^*_{xt} = \frac{1}{4}(\,|\,\mathbf{A}^*_{xt}\cdot\nabla_{xt}\mathbf{N}_{xti}\,|\,)^{-1} \tag{38}$$

or using the 2 matrix norm and the space–time Jacobian matrix $\mathbf{J}_{xt}$:

$$\mathbf{P}^*_{xt} = \frac{1}{4}(\|\mathbf{J}^{-1}_{xt}\mathbf{A}^*_{xt}\|_2)^{-1}. \tag{39}$$

Since the matrices $\mathbf{A}^*_t$, $\mathbf{A}^*_x$, $\mathbf{A}^*_y$, $\mathbf{A}^*_z$ that contribute to building $\mathbf{A}^*_{xt} = (\mathbf{A}^{*T}_t, \mathbf{A}^{*T}_x, \mathbf{A}^{*T}_y, \mathbf{A}^{*T}_z)^T$ are diagonal, the matrix $\mathbf{P}^*_{xt}$ is also diagonal. In the traditional Petrov–Galerkin method $\mathbf{A}^*_{xt} = \mathbf{A}_{xt}$ in the aforementioned expression and $\mathbf{P}_{xt}$ replaces $\mathbf{P}^*_{xt}$. The finite element space–time Jacobian matrix for 3D time dependent problems assumes the form:

$$\mathbf{J}_{xt} = \begin{pmatrix} \mathbf{I}\frac{1}{2}\Delta t & 0 & 0 & 0 \\ \mathbf{I}\frac{\partial y}{\partial t'}0 & \mathbf{I}\frac{\partial x}{\partial x'} & \mathbf{I}\frac{\partial y}{\partial x'} & \mathbf{I}\frac{\partial z}{\partial x'} \\ 0 & \mathbf{I}\frac{\partial x}{\partial y'} & \mathbf{I}\frac{\partial y}{\partial y'} & \mathbf{I}\frac{\partial z}{\partial y'} \\ 0 & \mathbf{I}\frac{\partial x}{\partial z'} & \mathbf{I}\frac{\partial y}{\partial z'} & \mathbf{I}\frac{\partial z}{\partial z'} \end{pmatrix}, \tag{40}$$

where the variables with $'$ are the local variables and where $\mathbf{I}$ is the $\mathcal{M}\times\mathcal{M}$ identity matrix in which $\mathcal{M}$ is the number of solution variables at each DG node, and $\Delta t$ is a time step size.

In a similar way to the scalar equation, the value of $\mathbf{P}^*_{xt}$ can be adjusted to ensure that the resulting value of $\mathbf{P}^*_{xt}$ is not so large to allow more transport backwards than forward in the resulting discrete system of equations using:

$$\mathbf{P}^*_{xt} = min\left\{\mathbf{E}^{-1}, \frac{1}{4}(\|\mathbf{J}^{-1}_{xt}\mathbf{A}^*_{xt}\|_2)^{-1}\right\}. \tag{41}$$

In this equation the diagonal entries of the matrix $\mathbf{E}$ are positive and $\mathbf{E}$ contains small positive numbers to avoid dividing by zero or near zero when one or more of the diagonals of $\mathbf{E}$ is zero or very small e.g. $1\times10^{-10}$.

We can work with the stabilization in diffusion form using the following equations:

$$\int_{V_E}\mathbf{N}_{xti}\mathbf{r}dV_E - \int_{\Gamma_E}\mathbf{N}_{xti}(\mathbf{n}_{xt}\cdot\mathbf{A}_{xt})(\Psi-\Psi_{bc})d\Gamma_E$$

$$+\int_{V_E}(\nabla_{xt}\mathbf{N}_{xti})^T\mathbf{K}\nabla_{xt}\mathbf{u}dV_E = \mathbf{0} \tag{42}$$

or in a form where we apply integration by parts of the transport terms once:

$$\int_{V_E}\mathbf{N}_{xti}(-\mathbf{s})dV - \int_{V_E}(\nabla_{xt}\cdot(\mathbf{N}_{xti}\mathbf{A}_{xt}))\Psi\,dV_E$$

$$+\int_{\Gamma_E}\mathbf{N}_{xti}(\mathbf{n}_{xt}\cdot\mathbf{A}_{xt})\Psi_{bc}\,d\Gamma_E + \int_{V_E}(\nabla_{xt}\mathbf{N}_{xti})^T\mathbf{K}\nabla_{xt}\Psi\,dV_E = \mathbf{0}, \tag{43}$$

in which the $\mathcal{M}\times\mathcal{M}$ diagonal matrix containing the diffusion coefficients is:

$$\mathbf{K} = \mathbf{V}(\mathbf{A}_{xt}\cdot\nabla_{xt}\mathbf{u})\mathbf{P}^*_{xt}\mathbf{V}(\|\nabla_{xt}\mathbf{u}\|_2^2)^{-1}\mathbf{V}(\mathbf{r}). \tag{44}$$

The resulting diagonal matrix $\mathbf{K}$ can be modified to ensure a non-negative diffusion by setting any of its negative entries to zero or by switching to their absolute values. Alternatively one can work with the residual only, by replacing $\mathbf{A}_{xt}\cdot\nabla_{xt}\mathbf{u}$ with the residual $\mathbf{r}$, which results in:

$$\mathbf{K}=\mathbf{V}(\mathbf{r})^T\mathbf{P}^*_{xt}\mathbf{V}(\|\nabla_{xt}\mathbf{u}\|_2^2)^{-1}\mathbf{V}(\mathbf{r}), \tag{45}$$

which is always positive since $\mathbf{P}^*_{xt}$ is positive semi-definite (as well as diagonal) and in which $\mathbf{V}(\mathbf{r})$ is the diagonal matrix containing the residual of the governing equations on its diagonal. Eq. (45) for the diffusivity can be derived by re-defining $\mathbf{A}^*_{xt}$ in Eq. (32) to:

$$\mathbf{A}^*_{xt}=\mathbf{V}(\mathbf{r})\mathbf{V}(\|\nabla_{xt}\mathbf{u}\|_2^2)^{-1}\nabla_{xt}\mathbf{u}. \tag{46}$$

### 4.2. The simplified Petrov–Galerkin Navier–Stokes equations

Assuming the two time level $\theta$-method is used for the discretisation of time:

$$\mathbf{r}=\mathbf{A}_t\frac{\mathbf{u}^{n+1}-\mathbf{u}^n}{\Delta t}+\mathbf{A}\cdot\nabla\mathbf{u}^{n+\theta}-\mathbf{s}^{n+\theta}, \tag{47}$$

with $\mathbf{A_x}=(\mathbf{A}_x\ \ \mathbf{A}_y\ \ \mathbf{A}_z)^T$, $\mathbf{s}^{\mathbf{n}+\theta}=-f\mathbf{k}\times\mathbf{u}^{n+\theta}-\nabla p^{n+\theta}+\nabla\cdot\boldsymbol{\tau}^{n+\theta}$, $\mathbf{u}^{n+\theta}=\Theta\mathbf{u}^{n+1}+(\mathbf{I}-\Theta)\mathbf{u}^n$, $p^{n+\theta}=\Theta p^{n+1}+(\mathbf{I}-\Theta)p^n$, and $\tau^{n+\theta}=\Theta\tau^{n+1}+(\mathbf{I}-\Theta)\tau^n$, in which $\Theta$ is a diagonal matrix containing the time stepping parameters, and $\mathbf{s}^{\mathbf{n}+\theta}=-f\mathbf{k}\times\mathbf{u}^{n+\theta}-\nabla p^{n+\theta}+\nabla\cdot\boldsymbol{\tau}^{n+\theta}$. Defining

$$\nabla_{xt}\mathbf{u}=\left(\frac{\mathbf{u}^{n+1}-\mathbf{u}^n}{\Delta t},\ (\nabla\mathbf{u}^{n+\theta})^T\right)^T, \tag{48}$$

enables the application of the formalism of space–time discretisation developed here, for example:

$$\mathbf{A}^*_{xt}=(\mathbf{A}^{*T}_t,\ \mathbf{A}^{*T}_{\mathbf{x}})^T=\mathbf{V}(\mathbf{A}_{xt}\cdot\nabla_{xt}\mathbf{u})\mathbf{V}(\|\nabla_{xt}\mathbf{u}\|_2^2)^{-1}\nabla_{xt}\mathbf{u} \tag{49}$$

and

$$\mathbf{P}^*_{xt}=min\left\{\mathbf{E}^{-1},\frac{1}{4}(\|\mathbf{J}^{-1}\mathbf{A}^*_{\mathbf{x}}\|_2)^{-1}\right\}, \tag{50}$$

in which $\mathbf{J}$ is the block part of the matrix $\mathbf{J}_{xt}$ that is associated with Cartesian space. By applying the diffusion only in Cartesian space the stabilized discrete equations in a diffusion form can be written:

$$\int_{V_E}\mathbf{N}_i\mathbf{r}dV-\int_{\Gamma_E}\mathbf{N}_i(\mathbf{n}\cdot\mathbf{A})\left(\Psi^{n+\theta}-\Psi^{n+\theta}_{bc}\right)d\Gamma_E+\int_{V_E}(\nabla\mathbf{N}_i)^T\mathbf{K}\nabla\mathbf{u}^{n+1}dV=\mathbf{0} \tag{51}$$

or in a form where we apply integration by parts:

$$\int_{V_E}\mathbf{N}_i\left(\mathbf{A}_t\frac{\Psi^{n+1}-\Psi^n}{\Delta t}-\mathbf{s}^{n+\theta}\right)dV_E-\int_{V_E}\nabla\cdot(\mathbf{N}_i\mathbf{A})\Psi^{n+\theta}dV+\int_{\Gamma_E}\mathbf{N}_i(\mathbf{n}\cdot\mathbf{A})\Psi^{n+\theta}_{bc}+\int_{\Gamma_E}\mathbf{N}_i(\mathbf{n}\cdot\mathbf{A})\Psi^{n+\theta}\,d\Gamma_E+\int_{V_E}(\nabla\mathbf{N}_i)^T\mathbf{K}\nabla\Psi^{n+1}\,dV_E=\mathbf{0}. \tag{52}$$

## 5. Petrov–Galerkin reduced order modelling

The Petrov–Galerkin method described above is used to form a stable POD reduced order model for nonlinear hybrid problems.

For simplicity, we assume the discretisation of the original Eqs. (1) and (2) at a given time step has the following form:

$$\mathbf{A}\Psi=\mathbf{b}, \tag{53}$$

where $\Psi=(\mathbf{U},\mathbf{V},\mathbf{W},\mathbf{P})^T$, $\mathbf{U}=(u_1,\ldots,u_i,\ldots,u_{\mathcal{N}})$, $\mathbf{V}=(\mathbf{v_1},\ldots,\mathbf{v_i},\ldots,\mathbf{v}_{\mathcal{N}})$, $\mathbf{W}=(\mathbf{w_1},\ldots,\mathbf{w_i},\ldots,\mathbf{w}_{\mathcal{N}})$ and $\mathbf{P}=(p_1,\ldots,p_i,\ldots,p_{\mathcal{N}})$ ($\mathcal{N}$ is the number of nodes in the computational domain). The modified system of Eq. (53) can then be written:

$$\mathbf{C}^T\mathbf{F}^{-1}\mathbf{A}\Psi=\mathbf{C}^T\mathbf{F}^{-1}\mathbf{b}, \tag{54}$$

in which for the least squares (LS) methods, $\mathbf{C}=\mathbf{A}$. Notice that the solution of this Eq. (54) is the same as that of Eq. (53), however critically it is not the same when the reduced order modelling is applied. The weighting matrix $\mathbf{F}$ can be chosen in order to render the system of equations dimensionally consistent (and thus may contain characteristic dimensions such as the time step size $\Delta t$ and a length scale) and also contain the mass matrix of the system. The LS methods have dissipative properties, unlike Galerkin methods, but are not generally conservative for coupled systems of equations. However the (LS) methods may be applied at each equation level to render them conservative, in which case $\mathbf{C}$ may contain just parts of the matrix $\mathbf{A}$.

However, the above mechanics can also be applied to form conservative stabilization methods for ROMs which for non-linear problems have a tendency to diverge due to inadequate sub-grid-scale modelling (if Galerkin methods are applied e.g. the POD method). A common solution to the divergence of ROM solutions is to add diffusion terms to the equations and tune these diffusion terms to best match the full forward solution. Thus, it seems natural to explore the Petrov–Galerkin methodology in order to introduce diffusion into ROMs and avoid this tuning.

The matrix equation (53) can now be converted into a reduced order system that is spanned by a set of $m$ POD basis functions denoted by $\{\Phi_1,\ldots,\Phi_M\}$. Each POD function is represented by a vector of size $\mathcal{N}$ that represents the functions over the finite element space. The POD functions are grouped together into a matrix $\mathbf{M}^{POD}$ which is of size $\mathcal{N}\times\mathcal{M}$ and given by $\mathbf{M}^{POD}=[\Phi_1,\ldots,\Phi_M]$. Using this matrix, the reduced order system can now be generated by operating directly on the discretised linear system given in Eq. (53). That is, a standard Galerkin approach is applied, whereby the full system is pre and post multiplied by $\mathbf{M}^{POD^T}$ and $\mathbf{M}^{POD}$, respectively. The resulting reduced order system results,

$$\mathbf{M}^{POD^T}\mathbf{A}\mathbf{M}^{POD}\Psi^{POD}=\mathbf{M}^{POD^T}(\mathbf{b}-\mathbf{A}\bar{\Psi}), \tag{55}$$

where $\Psi^{POD}$ are the reduced order solution coefficients, $\bar{\Psi}$ is the mean of the variables $\Psi$ over the time, and the relationship between the pod variables and full solutions is given by,

$$\Psi=\mathbf{M}^{POD^T}(\Psi^{POD}+\bar{\Psi}). \tag{56}$$

For LS methods, Eq. (55) is:

$$\mathbf{M}^{POD^T}\mathbf{C}^T\mathbf{F}^{-1}\mathbf{A}\mathbf{M}^{POD}\Psi^{POD}=\mathbf{M}^{POD^T}\mathbf{C}^T\mathbf{F}^{-1}(\mathbf{b}-\mathbf{A}\bar{\Psi}) \tag{57}$$

and using the non-linear Petrov–Galerkin methods described above:

$$\mathbf{M}^{POD^T}(\mathbf{I}+\mathbf{C}^T\mathbf{F}^{-1})\mathbf{A}\mathbf{M}^{POD}\Psi^{POD}=\mathbf{M}^{POD^T}(\mathbf{I}+\mathbf{C}^T\mathbf{F}^{-1})(\mathbf{b}-\mathbf{A}\bar{\Psi}) \tag{58}$$

or in a diffusion form (analogous to (42)–(44)):

$$\left(\mathbf{M}^{POD^T}\mathbf{A}\mathbf{M}^{POD}+\mathbf{D}\right)\Psi^{POD}=\mathbf{M}^{POD^T}(\mathbf{b}-\mathbf{A}\bar{\Psi}). \tag{59}$$

In Eq. (59) we have also introduced a diffusion matrix $\mathbf{D}$, which has the following form (where the surface integral is neglected since it has little effect on results):

$$\mathbf{D}=\begin{pmatrix}\mathbf{D}_u & 0 & 0 & 0\\ 0 & \mathbf{D}_v & 0 & 0\\ 0 & 0 & \mathbf{D}_w & 0\\ 0 & 0 & 0 & \mathbf{D}_p\end{pmatrix}, \tag{60}$$

$$\mathbf{D}_{umk} = \int_V \nabla N_{xt_m}^{POD} \mu_u^{POD} \nabla N_{xt_k}^{POD}\, dV, \tag{61}$$

$$\mathbf{D}_{vmk} = \int_V \nabla N_{xt_m}^{POD} \mu_v^{POD} \nabla N_{xt_k}^{POD}\, dV, \tag{62}$$

$$\mathbf{D}_{wmk} = \int_V \nabla N_{xt_m}^{POD} \mu_w^{POD} \nabla N_{xt_k}^{POD}\, dV, \tag{63}$$

$$\mathbf{D}_{pmk} = \int_V \nabla N_{xt_m}^{POD} \mu_p^{POD} \nabla N_{xt_k}^{POD}\, dV, \tag{64}$$

where the $N_{xt_k}^{POD}$ basis functions are interpolated using the finite element basis functions. the diffusion coefficient in $\mathbf{D}$ can be calculated using (analogous to (22)):

$$\left(\mu_u^{POD} \;\; \mu_v^{POD} \;\; \mu_w^{POD} \;\; \mu_p^{POD}\right)^T = \frac{r^{POD} p_{xt}^{*POD} r^{POD}}{\left\|\nabla_{xt}\psi^{POD}\right\|_2^2}, \tag{65}$$

in the present work, the diffusion terms are only applied to the momentum equations, so that $p^{POD} = 0$, $p_{xt}^{*POD}$ is calculated:

$$p_{xt}^{*POD} = min_k\left\{\frac{1}{4}(\mid \mathbf{a}_{xt}^* \cdot \nabla_{xt} N_{xtk} \mid)^{-1}\right\} \tag{66}$$

or using the POD basis function:

$$p_{xt}^{*POD} = min_k\left\{\frac{1}{4}(\mid \mathbf{a}_{xt}^* \cdot \nabla_{xt} N_{xtk}^{POD} \mid)^{-1}\right\}. \tag{67}$$

The residual vector can be determined from:

$$\mathbf{r}^{POD} = \mathbf{E}^{POD-1}\left(\left(\mathbf{M}^{POD^T}\mathbf{A}\mathbf{M}^{POD}\right)\Psi^{POD} - \mathbf{M}^{POD^T}(\mathbf{b} - \mathbf{A}\bar{\Psi})\right) \tag{68}$$

or since the absolute value of the residual may not matter:

$$\mathbf{r}^{POD} = \mathbf{E}^{POD^{-1}}\mathbf{M}^{POD^T} \mid \mathbf{A}\mathbf{M}^{POD}\Psi^{POD} - (\mathbf{b} - \mathbf{A}\bar{\Psi}) \mid, \tag{69}$$

where $\mathbf{E}_{ij}^{POD} = \int_V \Psi_i^{POD}\Psi_j^{POD}\, dV$. Taking into account the ROM basis functions are orthonormal, so that $\mathbf{E}^{POD} = \mathbf{I}$.

## 6. Application cases and numerical results

The Petrov–Galerkin method has been applied into a finite element fluids model (Fluidity, developed by the Applied Modelling and Computation Group at Imperial College London) to explore the stability and accuracy of reduced order modelling in the two test cases: a gyre case and the flow past a cylinder case. In order to compare the results obtained by either the Galerkin or the Petrov–Galerkin method, Reynolds numbers are set with 2000 and 3600 for a flow past a cylinder and 10,000 for a Gyre.

This paper presents results using both a mixed finite element pair $P_{1DG}P_2$ and a $P_1P_1$ formulation. The $P_1P_1$ element type has been included in the analysis due to it being a popular element choice, however it can in many instances cause solutions to become unstable as it is a LBB unstable element. In this work, the $P_1P_1$ element is stabilised by explicitly adding a fourth order stabilization term in pressure into the continuity equation, as described in Pain et al. [37].

Fig. 1 shows the two dimensional $P_{1DG}P_2$ element which has three local nodes associated with velocity and six associated with pressure. The velocity variation is discontinuous between elements and the pressure variable is continuous. The advantage of this particular element choice is that the mass matrix for velocity is a block diagonal matrix so that it can be trivially inverted; also it allows the order of the pressure to be increased to quadratic whilst maintaining LBB stability [38]. This element also has the ability represent very accurately the balance between the pressure or free surface gradients and the Coriolis force as well as buoyancy forces.

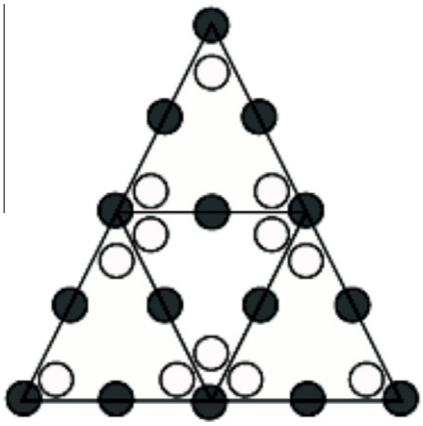

**Fig. 1.** A mixed finite element $P_{1DG}P_2$ pair for velocity and pressure (white one for $u$ nodes, black one for $p$ nodes).

The root mean square error (RMSE) and correlation coefficient of results between the POD and full model at the time level $n$ are used to estimate the divergence of POD projection results:

$$RMSE^n = \sqrt{\frac{\sum_{i=1}^{\mathcal{N}}\left(\psi_i^n - \psi_{o,i}^n\right)^2}{\mathcal{N}}}, \tag{70}$$

where, $\psi_i^n$ and $\psi_{o,i}^n$ are the vectors containing the POD and full model results at the node $i$ respectively. $\mathcal{N}$ represents number of nodes. The correlation coefficient of results between the POD and full models at the time level $n$ with expected values $\mu_{\psi^n}$ and $\mu_{\psi_o^n}$ and standard deviations $\sigma_{\psi^n}$ and $\sigma_{\psi_o^n}$ is defined as:

$$corr(\psi^n, \psi_o^n)^n = \frac{cov(\psi^n, \psi_o^n)}{\sigma_{\psi^n}\sigma_{\psi_o^n}} = \frac{E(\psi^n - \sigma_{\psi^n})(\psi_o^n - \sigma_{\psi_o^n})}{\sigma_{\psi^n}\sigma_{\psi_o^n}}. \tag{71}$$

### 6.1. Case 1: flow past a cylinder

The non-dimensional 2D case is composed of a cylinder with a radius of 3 in the computational domain (50 long and 10 wide). An inlet boundary with a velocity of 1 (non-dimensional) flows parallel to the domain length towards the right of the domain. The centre of the cylinder is placed 5 (non-dimensional) units from the inlet boundary. The Reynolds number ($Re$) are 2000 and 3600. Dirichlet boundary conditions are applied to the cylinder and no normal flow and zero shear (slip) boundary conditions are applied to both lateral sides. The simulation period is $[0 - 10]$ with a time step size of $\Delta t = 0.02$. The solution at $t = 2.4$ and $t = 7$ over the period $[0 - 10]$ are chosen to show the effects. In order to show stabilisation of Petrov–Galerkin method for Reduced order model, 50 snapshots and 22 POD basis functions which capture 99% percent of energy are chosen for $u$, $v$ and $p$. Fig. 2 shows the results of full model using a $P_1P_1$ element type, together with the POD/Galerkin and POD/Petrov–Galerkin models for Reynolds number 2000. Both POD models have a reasonable qualitative agreement with the full model for this Reynolds number.

Then the Reynolds number is increased until POD/Galerkin crashes. Fig. 3 shows the velocity field (vector) obtained from the full model (using $P_1P_1$ element type) and POD models using the Galerkin and Petrov–Galerkin methods. The Reynolds number is

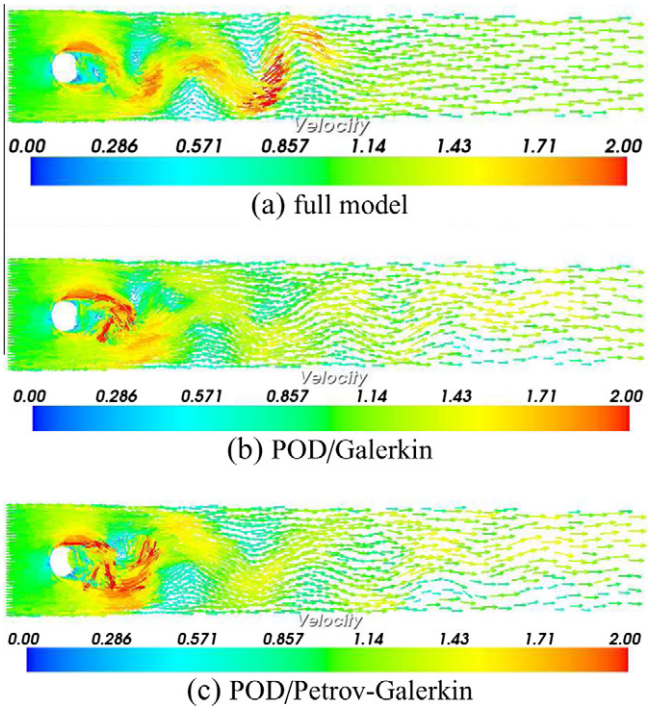


**Fig. 2.** Flow past a cylinder: velocity solution from the full, POD/Galerkin and POD/Petrov–Galerkin models using $P_1P_1$ ($t = 3.6$, $Re = 2000$).

3600. It can be seen in Fig. 3(c) and (d) that the results of reduced order model (ROM) using Galerkin method become unstable (the solution of velocity is too large, 29.2 when $t = 2.4$ and 113 when $t = 7$. A variable colour legend is chosen to show the large velocity value), while the results of ROM using Petrov–Galerkin method are considerably more stable.

In order to further investigate the stability and accuracy of the new Petrov–Galerkin method in ROM, the velocity solution at a specified detector in cylinder is plotted in Fig. 4. It shows that the difference of velocity results between the full model and the POD model solution using Petrov–Galerkin methods is rather small.

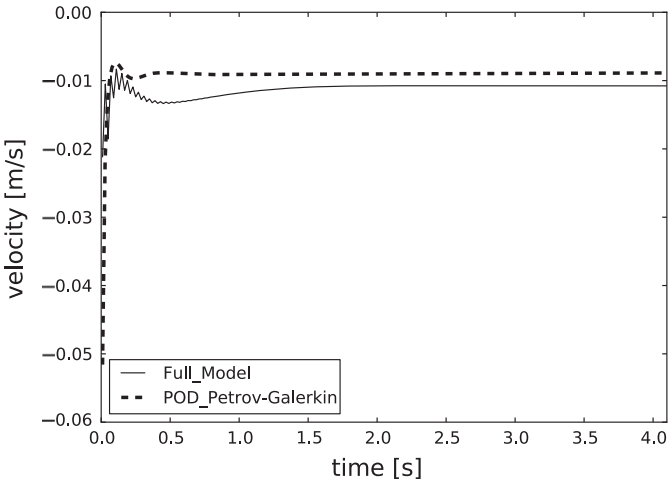


**Fig. 4.** Comparison of velocity results between the full and Petrov–Galerkin POD models at a point (near right side of the circle).

A mixed $P_{1DG}P_2$ finite element pair is introduced here to further stabilise the numerical oscillation, which consists of discontinuous linear elements for velocity and continuous quadratic elements for pressure. Fig. 5 presents a comparison of the velocity solutions using the full and POD models with a mixed $P_{1DG}P_2$ finite element pair. The Reynolds number is 3600. Fig. 6 shows the comparison of velocity value between the full model, the POD/Galerkin model and POD/Petrov–Galerkin model at point ($x = 0.3$ and $y = 0.3$) along whole domain (reference coordinate system: $0 \leqslant x \leqslant 2.2$ and $0 \leqslant y \leqslant 0.41$). It can be seen that the POD results using the Galerkin method are unstable while those from the POD/

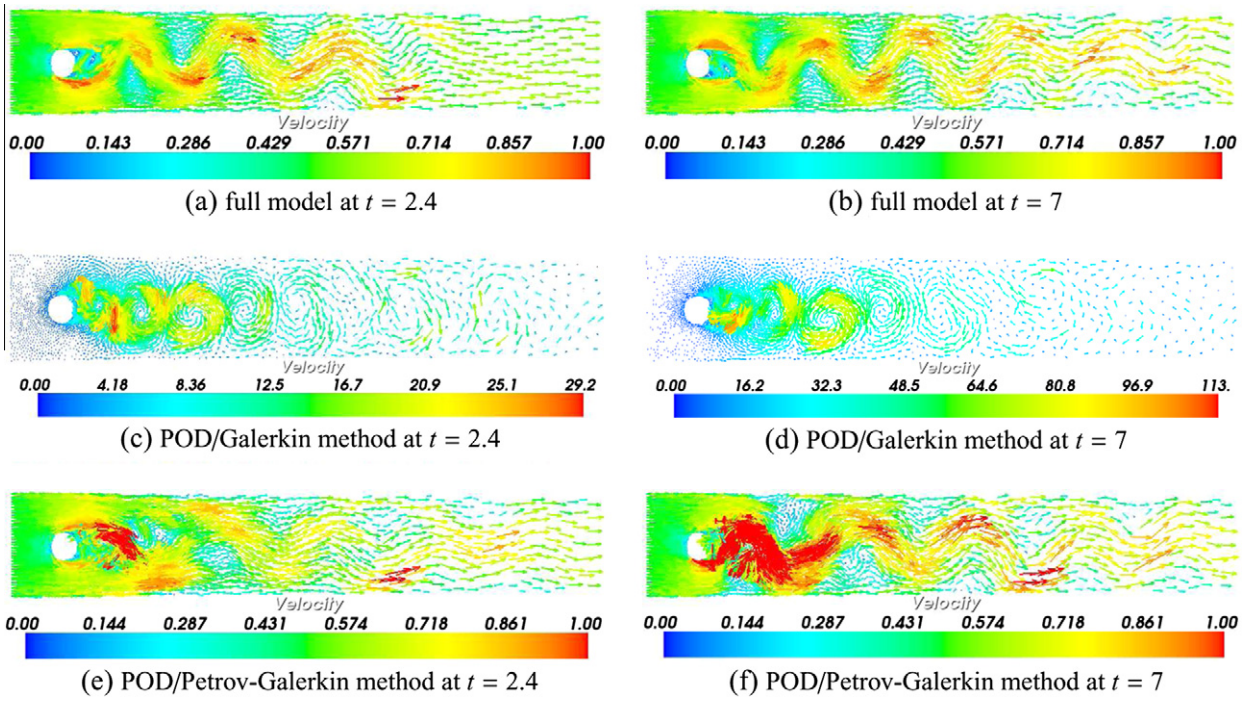


**Fig. 3.** Flow past a cylinder: Velocity solution from the full, POD/Galerkin and POD/Petrov–Galerkin models using $P_1P_1$ at $t = 2.4$and $t = 7$ ($Re = 3600$).

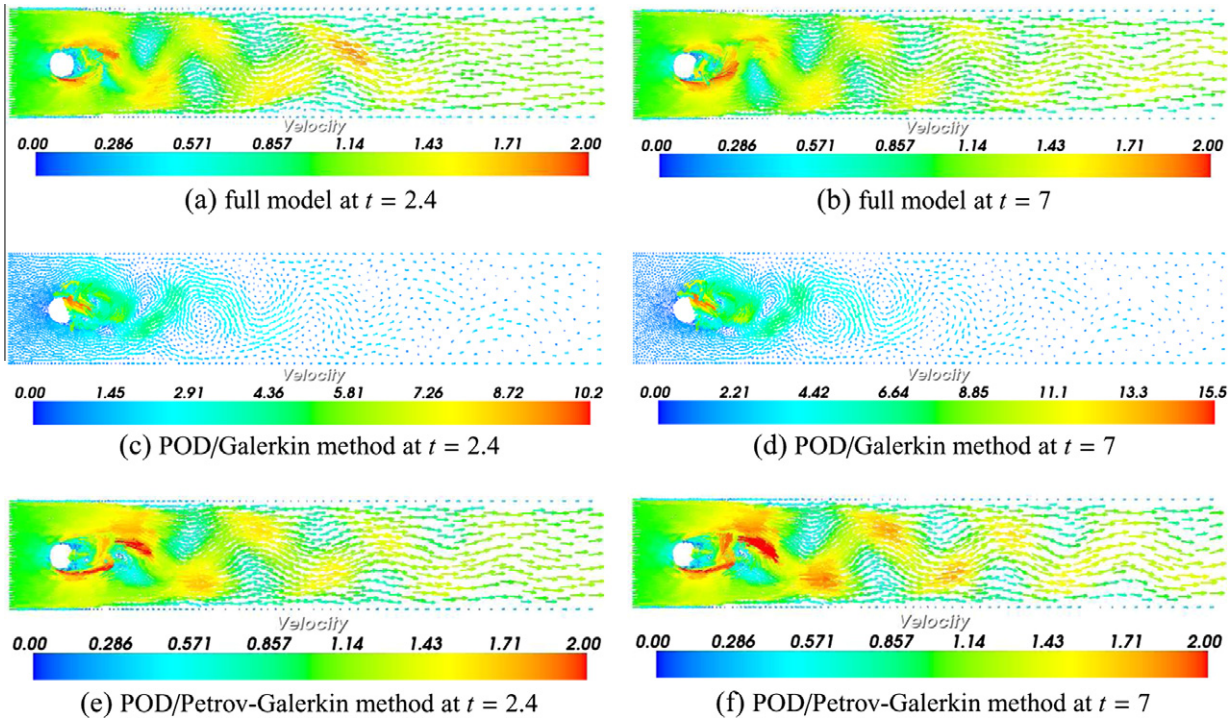


**Fig. 5.** Flow past a cylinder: solution of full model, POD/Galerkin and POD/Petrov–Galerkin using $P_{1DG}P_2$ at $t = 2.4$ and $t = 7$ ($Re = 3600$).

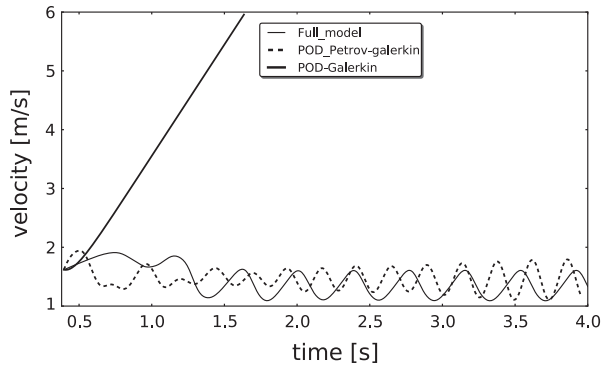


**Fig. 6.** The comparison of velocity solution at point ($x = 0.3$, $y = 0.3$) between the Galerkin/POD model and Petrov–Galerkin/POD model using $P_{1DG}P_2$.

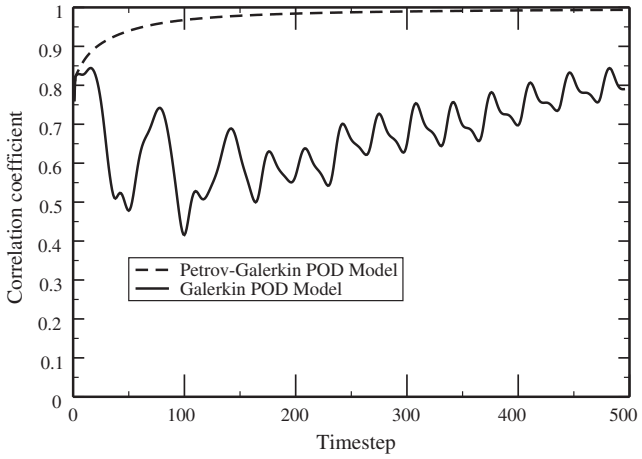


**Fig. 7.** The correlation coefficient of the Galerkin/POD and Petrov–Galerkin/POD models using a mixed finite element $P_{1DG}P_2$ pair for velocity and pressure.

Petrov–Galerkin model are stable. Fig. 7 shows the correlation coefficient of results between the POD and full models can achieve from 80% for the traditional Galerkin POD model to 98% if the Petrov–Galerkin approach is used.

### 6.2. Case 2: gyre

The Petrov–Galerkin reduced order model is also tested in a Gyre problem in a computational domain of horizontal dimensions, 1000 km by 1000 km with a depth of $H$ 500 m. The wind forcing on the free surface is given by

$$\tau_y = \tau_0 cos(\pi y/L), \quad \tau_x = 0.0, \tag{72}$$

where $\tau_x$ and $\tau_y$ are the wind stresses on the free surface along the $x$ and $y$ directions respectively, and $L = 1000$ km. A maximum zonal wind stress of $\tau_0 = 0.1$ N m$^{-1}$ is applied in the latitude ($y$) direction. $\beta = 1.8 \times 10^{-11}$ and the reference density $\rho_0 = 1000$ kg m$^{-1}$ were used. In this case, The simulation period is $[0 - 0.6]$ with a time step size of $\Delta = 0.01$. 60 snapshots and 25 POD basis functions which capture 99% of energy are chosen for $u$, $v$ and $p$. In order to investigate the effects of the new Petrov–Galerkin method, the Reynolds number is increased until the results of ROM using the Galerkin method become unstable or crash. The Reynolds number is chosen to be 10,000. Dirichlet weakly boundary conditions are applied. Fig. 8 shows the velocity solution at $t = 0.35$ become very large and stable while the results of Petrov–Galerkin $P_{1DG}P_2$ are considerably more stable.

Fig. 9 shows the RMSE between the full and POD model using the Galerkin method and Petrov–Galerkin method. In order to see clearly the RMSE between Petrov–Galerkin and full model,

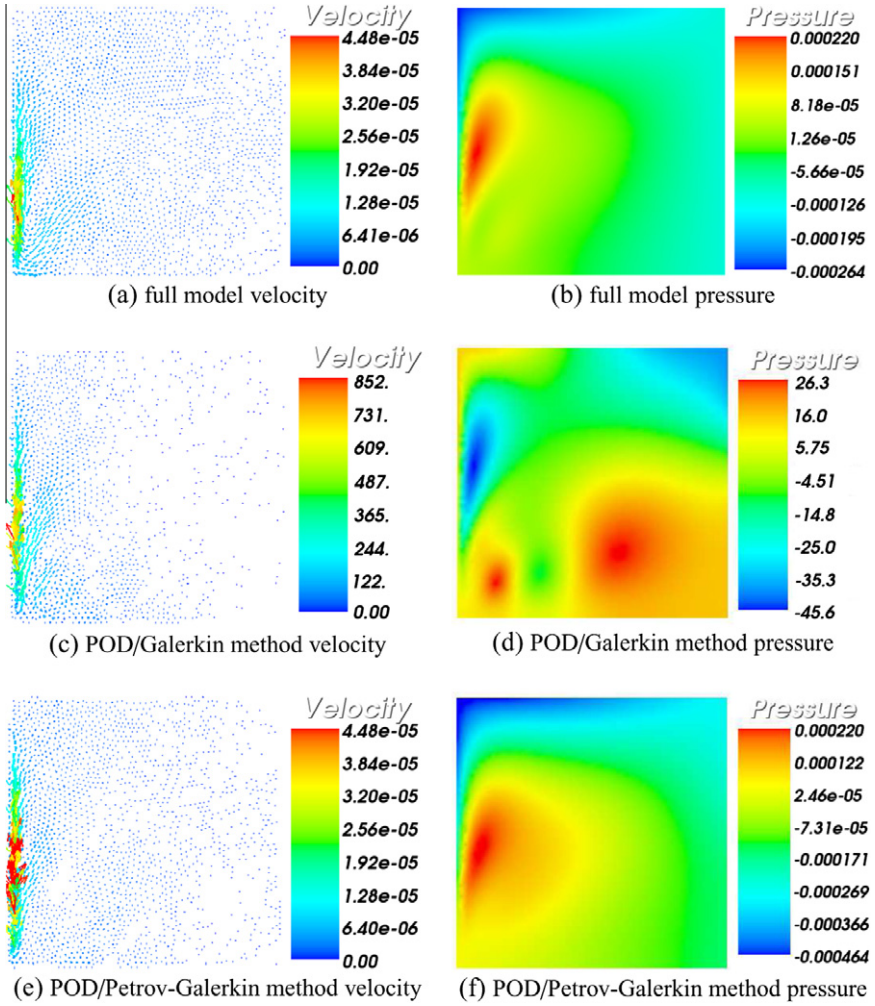


**Fig. 8.** Gyre: comparison of the results between the full and POD models at $t = 0.35$ using $P_{1DG}P_2$.

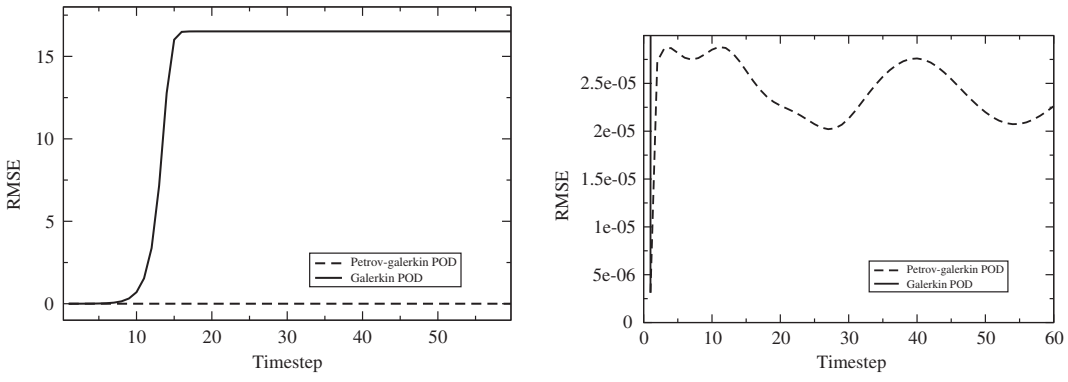


**Fig. 9.** Gyre: RMSE between full model and POD model.

the Fig. 9(a) is enlarged into Fig. 9(b). From the value of $y$ axis, the RMSE between Petrov–Galerkin with full model is much smaller than the RMSE between Galerkin method and full model. The RMSE between the full and POD models is decreased by 90%. The divergence of Galerkin/POD is well controlled by the new Petrov–Galerkin/POD.

It can be seen from Figs. 9 and 10 that the POD reduced order results using the Galerkin approach become oscillatory and unstable and the RMSE of results increases as the simulation time increases. By using the Petrov–Galerkin POD approach, the RMSE of results is reduced while the correlation coefficient increases to 99.99% after a few time steps.

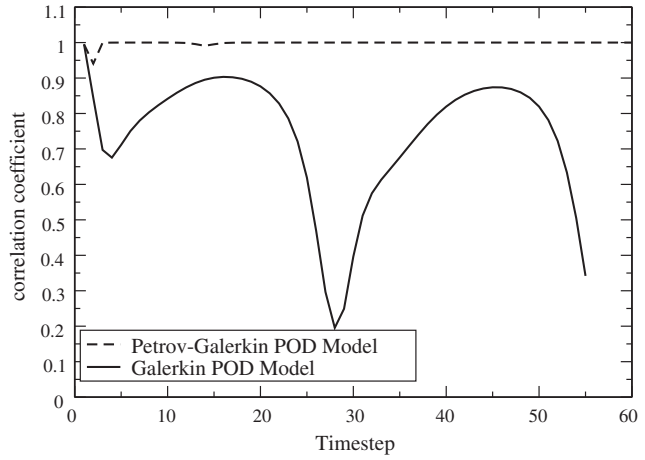


**Fig. 10.** Correlation coefficient of Galerkin/POD model and Petrov–Galerkin/POD model.

**Table 1**
Comparison of CPU (unit: s) required for running the full model and ROM for each time step.

| Case | Model | Assembling matrices | Solving | Projecting back | Total |
|---|---|---|---|---|---|
| Case 1 | Full model | 3.00373 | 0.112598 | 0.0000 | 3.116328 |
| | POD ROM | 0.30280 | 0.000000 | 0.0199 | 0.322700 |
| Case 2 | Full model | 2.96455 | 0.103687 | 0.0000 | 3.068237 |
| | POD ROM | 0.29875 | 0.000000 | 0.0193 | 0.318050 |

Table 1 shows the CPU time of main process at each time step. It can be seen that once the POD model is setup (involving assembling the matrices process), the reduced order model saves 90% of CPU time required by the full model.

## 7. Summary and conclusions

A new non-linear Petrov–Galerkin method for reduced order Navier–Stokes equations using a mixed continuous/discontinuous finite element pair has been presented. This method is used to stabilise the reduced order Navier–Stokes equations. The method has been implemented in a finite element adaptive mesh refinement fluids model (Fluidity) and applied to a Gyre and flow past a cylinder test cases.

The effect of the new non-linear Petrov–Galerkin method on stabilisation of the POD model is evaluated through comparison of results between the POD model using the Petrov–Galerkin method and the traditional Galerkin/POD model. The results show that the Galerkin/POD model becomes oscillatory and unstable as the Reynolds number increases over a certain value. By introducing Petrov–Galerkin method in reduced order modelling, the stability of the results is maintained.

An error analysis has also been carried out for the validation and accuracy of the new POD/Petrov–Galerkin model. The RMSE of results between the POD and Full model is decreased while the correlation coefficient is mostly larger than 99%–99.5%. The new POD/Petrov–Galerkin model does well in flow past a cylinder and gyre problems. Future work will investigate the effects of applying this new Petrov–Galerkin/POD approach to more complex fluid flow models.

## Acknowledgements

This work was undertaken at AMCG, Imperial College London, with support from the UK's Natural Environment Research Council (Projects NER/A/S/2003/00595, NE/C52101X/1, NE/J015938/1 and NE/C51829X/1), the Engineering and Physical Sciences Research Council (GR/R60898, EP/I00405X/1 and EP/J002011/1), and the Imperial College High Performance Computing Service. Prof. I.M. Navon acknowledges the support of NSF/CMG Grant ATM-0931198. Dunhui Xiao acknowledges the support of China Scholarship Council. The authors acknowledge the reviewers and Editor for their in depth perspicacious comments that contributed to improving the presentation of this paper. Andrew Buchan wishes to acknowledge the EPSRC for funding his contribution to this article through the Grant Ref.: EP/J002011/1. Drs. Fang and Du would like to acknowledge the EPSRC international research collaboration funding. Juan Du would like to acknowledge China Postdoctoral Science Foundation with Grant No. 2012M520361.

## References

[1] K. Pearson, On lines and planes of closest fit to systems of points in space, Philos. Mag. 2 (1901) 559–572.
[2] D.D. Kosambi, Statistics in function space, J. Indian Math. Soc. 7 (1943) 76–88.
[3] K. Fukunaga, Introduction to Statistical Recognition, second ed., Computer Science and Scientific Computing Series, Academic Press, Boston, MA, 1990.
[4] I.T. Jolliffe, Principal Component Analysis, second ed., Springer, 2002.
[5] D.T. Crommelin, A.J. Majda, Strategies for model reduction: comparing different optimal bases, J. Atmos. Sci. 61 (2004) 2206–2217.
[6] N. Aubry, P. Holmes, J.L. Lumley, The dynamics of coherent structures in the wall region of a turbulent boundary layer, J. Fluid Dynam. 192 (1998) 115–173.
[7] K. Kunisch, S. Volkwein, Galerkin proper orthogonal decomposition methods for a general equation in fluid dynamics, SIAM J. Numer. Anal. 40 (2003) 492–515.
[8] Z. Luo, J. Zhu, R. Wang, I.M. Navon, Proper orthogonal decomposition approach and error estimation of mixed finite element methods for the tropical pacific ocean reduced gravity model, Comput. Methods Appl. Mech. Engrg. 196 (2007) 4184–4195.
[9] J.L. Lumley, The structure of inhomogeneous turbulence, Atmos. Turbul. Wave Propag. (1967) 166–178.
[10] N. Aubry, P. Holmes, J.L. Lumley, The dynamics of coherent structures in the wall region of a turbulent boundary layer, J. Fluid Dynam. 192 (1988) 115–173.
[11] K. Willcox, J. Peraire, Balanced model reduction via the proper orthogonal decomposition, AIAA J. 40 (2002) 2323–2330.
[12] H.T. Banks, M.L. Joyner, B. Wincheski, W.P. Winfree, Nondestructive evaluation using a reduced-order computational methodology, Inverse Probl. 16 (2000) 929–945.
[13] P.O. Hopcroftand, K. Gallagher, C.C. Pain, F. Fang, Three-dimensional simulation and inversion of borehole temperatures for reconstructing past climate in complex settings, J. Geophys. Res. (2009) 114.
[14] C. Robert, S. Durbiano, E. Blayo, J. Verron, J. Blum, F.X.L. Dimet, A reduced-order strategy for 4D-Var data assimilation, J. Marine Syst. 57 (2005) 70–82.
[15] Y. Cao, J. Zhu, I.M. Navon, Z. Luo, A reduced order approach to four-dimensional variational data assimilation using proper orthogonal decomposition, Int. J. Numer. Methods Fluids 53 (2007) 1571–1583.
[16] I. Hoteit, A. Kohl, Efficiency of reduced-order, time-dependent adjoint data assimilation approaches, J. Oceanogr. 62 (2006) 539–550.
[17] F. Fang, C.C. Pain, I.M. Navon, M.D. Piggott, G.J. Gorman, P. Allison, A.J.H. Goddard, Reduced order modelling of an adaptive mesh ocean model, Int. J. Numer. Methods Fluids 59 (2009) 827–851.
[18] L.P. Franca, S. Frey, Stabilized finite element methods: II. The incompressible Navier–Stokes equations, Comput. Methods Appl. Mech. Engrg. 99 (1992) 209–233.
[19] I. Kalashnikova, M.F. Barone, On the stability and convergence of a Galerkin reduced order model (ROM) of compressible flow with solid wall and far-field boundary treatment, Int. J. Numer. Methods Engrg. 00 (2009) 1–28.
[20] A. Iollo, S. Lanteri, J.A. Desideri, Stability properties of POD/Galerkin approximations for the compressible Navier–Stokes equations, Theor. Comput. Fluid Dynam. 13 (2000) 377–396.
[21] A. Iollo, A. Dervieux, J.A. Desideri, S. Lanteri, Two stable POD-based approximations to the Navier–Stokes equations, Comput. Visual. Sci. 3 (2000) 61–66.
[22] F. Sabetghadam, A. Jafarpour, $\alpha$ regularization of the POD–Galerkin dynamical systems of the Kuramoto–Sivashinsky equation, Appl. Math. Comput. 218 (2012) 6012–6026.
[23] S. Chaturantabut, D.C. Sorensen, Nonlinear model reduction via discrete empirical interpolation, SIAM J. Sci. Comput. 32 (2010) 2737–2764.

[24] M. Barrault, Y. Maday, N.C. Nguyen, A.T. Patera, An empirical interpolation method: application to efficient reduced-basis discretization of partial differential equations, C.R. Acad. Sci. Paris Ser. 339 (2004) 667–672.
[25] S. Chaturantabut, Dimension reduction for unsteady nonlinear partial differential equations via empirical interpolation methods, Master Thesis, Rice University, 2008.
[26] S. Chaturantabut, Nonlinear model reduction via discrete empirical interpolation, Ph.D. Thesis, Rice University, 2011.
[27] S. Chaturantabut, D.C. Sorensen, Application of POD and DEIM on dimension reduction of non-linear miscible viscous fingering in porous media, Math. Comput. Model. Dynam. Syst. 17 (2011) 337–353.
[28] S. Chaturantabut, D.C. Sorensen, A state space error estimate for POD–DEIM nonlinear model reduction, SIAM J. Numer. Anal. 50 (2012) 46–63.
[29] N.C. Nguyen, A.T. Patera, J. Peraire, A best points interpolation method for efficient approximation of parametrized functions, Int. J. Numer. Methods Engrg. 73 (2008) 521–543.
[30] N.C. Nguyen, J. Peraire, An efficient reduced-order modeling approach for non-linear parametrized partial differential equations, Int. J. Numer. Methods Engrg. 76 (2008) 27–55.
[31] M.A. Grepl, Y. Maday, N.C. Nguyen, A.T. Patera, Efficient reduced-basis treatment of nonaffine and nonlinear partial differential equations, Math. Model. Numer. Anal. 41 (2007) 575–605.
[32] K. Carlberg, C. Bou-Mosleh, C. Farhat, Efficient non-linear model reduction via a least-squares Petrov–Galerkin projection and compressive tensor approximations, Int. J. Numer. Methods Engrg. 86 (2011) 155–181.
[33] Y. Chu, M. Serpas, J. Hahn, State-preserving nonlinear model reduction procedure, Chem. Eng. Sci. 66 (2011) 3907–3913.
[34] F. Fang, C. Pain, I.M. Navon, A.H. Elsheikh, J. Du, D. Xiao, Non-linear Petrov–Galerkin methods for reduced order hyperbolic equations and discontinuous finite element methods, J. Comput. Phys. 234 (2013) 540–559.
[35] C.J. Cotter, D.A. Ham, C.C. Pain, A mixed discontinuous/continuous finite element pair for shallow-water ocean modelling, Ocean Model. 26 (2009) 86–90.
[36] C.J. Cotter, D.A. Ham, Numerical wave propagation for the triangular $P_{1DG}P_2$ finite element pair, J. Comput. Phys. 230 (2011) 2806–2820.
[37] C.C. Pain, A.P. Umpleby, C.R.E. de Oliveira, A.J.H. Goddard, Tetrahedral mesh optimisation and adaptivity for steady-state and transient finite element calculations, Comput. Methods Appl. Mech. Eng. 190 (2001) 3771–3796.
[38] C.J. Cotter, D.A. Ham, C.C. Pain, S. Reich, LBB stability of a mixed Galerkin finite element pair for fluid flow simulations, J. Comput. Phys. 228 (2009) 336–348.
[39] J. Du, F. Fang, C.C. Pain, I.M. Navon, J. Zhu, D.A. Ham, POD reduced-order unstructured mesh modeling applied to 2D and 3D fluid flow, Comput. Math. Appl. (2012), in press. http://dx.doi.org/10.1016/j.camwa.2012.06.009.
[40] T.J.R. Hughes, M. Mallet, A new finite element formulation for computational fluid dynamics: III. The generalized streamline operator for multidimensional advective–diffusive systems, Comput. Methods Appl. Mech. Engrg. 58 (1986) 305–328.
[41] T.J.R. Hughes, M. Mallet, A new finite element formulation for computational fluid dynamics: IV. A discontinuity-capturing operator for multidimensional advective–diffusive systems, Comput. Methods Appl. Mech. Engrg. 58 (1986) 329–336.
[42] A.N. Brooks, T.J.R. Hughes, Streamline upwind/Petrov–Galerkin formulations for convection dominated flows with particular emphasis on the incompressible Navier–Stokes equations, Comput. Methods Appl. Mech. Engrg. 32 (1982) 199–259.
[43] R. Codina, A discontinuity-capturing crosswind-dissipation for the finite element solution of the convection–diffusion equation, Comput. Methods Appl. Mech. Engrg. 110 (1993) 325–342.
[44] C.C. Pain, M.D. Eaton, R.P. Smedley-Stevenson, et al., Space–time streamline upwind Petrov–Galerkin methods for the Boltzmann transport equation, Comput. Methods Appl. Mech. Engrg. 195 (2006) 4334–4357.